Resonances and Nonuniformities in CMUT Elements or Arrays

Abdullah Atalar, and Hayrettin Köymen

Bilkent University, Electrical and Electronics Engineering Department, Ankara, Turkey

Email: aatalar@bilkent.edu.tr, koymen@ee.bilkent.edu.tr

Abstract—We determine the response of individual cells of a CMUT array immersed in water using the small-signal equivalent circuit of a single cell and radiation impedances. Using a numerically efficient technique, we are able to simulate large arrays. The results indicate the presence of resonances at low frequencies where Rayleigh-Bloch waves are excited on the surface of the array. Reflections from the edges cause standing-wave patterns. Above the cut-off frequency of Rayleigh-Bloch waves, no standing-wave pattern exists. However, there is nonuniformity among cell velocities mainly due to unequal radiation impedance seen by the cells. Rayleigh-Bloch waves and nonuniformity in cell velocities do not cause a significant degradation in the point spread function, but the oscillations extend the duration of impulse response, limiting the dynamic range.

I. INTRODUCTION

A typical CMUT probe consists of many CMUT cells placed side by side in a compact manner to generate more and directive acoustic power. It was shown that mutual interactions between the cells in such multi-cell configurations play a significant role in the velocity response of the cells [1]–[3]. The mutual coupling between two cells through the immersion medium manifests itself as the mutual acoustic impedance between those cells [4]. Since an individual CMUT cell has a low acoustic impedance, its response is mainly determined by the total (self and mutual) acoustic impedance imposed on the cell.

Analysis of infinitely large CMUT arrays [5] indicated presence of spurious surface waves. Infinite quasi-periodic CMUT structures were analyzed [6] predicting a slow dispersive wave at low frequencies due to cross-talk between the cells. An analytical method taking care of higher order plate modes was implemented to predict the response of a group of CMUT cells [7]. This method was limited to a relatively small number of cells, because of the large number of unknowns.

Previous methods failed to provide solutions for realistic finite-size CMUT arrays, either because the method required an infinite array or the number of unknowns was too large. In this paper, we show how to model an element or an array of large number of N CMUT cells immersed in a liquid. We use the small-signal equivalent circuit of a single cell modelling only the fundamental plate mode. The cells are biased with a DC voltage and excited with a sinusoidal source. We take care of the self-radiation impedance of the cell analytically and the mutual radiation impedances created by the neighboring cells using an approximate analytical expression to reduce the computation time. The resulting set of N linear equations with

N unknowns can be solved to find all cell velocities as a function of the excitation frequency.

II. MODELLING AN ARRAY OF CMUT CELLS

We consider an array of circular CMUT cells each with a cross-section shown in Fig. 1. The cells have a radius of a with full electrodes, a plate thickness of t_m and an effective gap
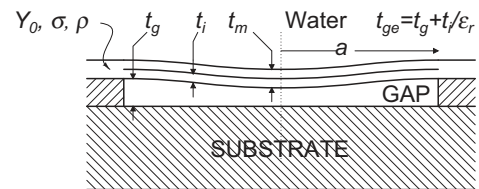

Fig. 1. Cross sectional view of a CMUT cell of radius a with full electrode.

height of t_{ge} and are biased with V_{DC}. They are arranged in a rectangular array in m elements each containing n identical circular cells placed in a flat rigid baffle and are immersed in water. Referring to Fig. 2, each CMUT cell is modelled by its
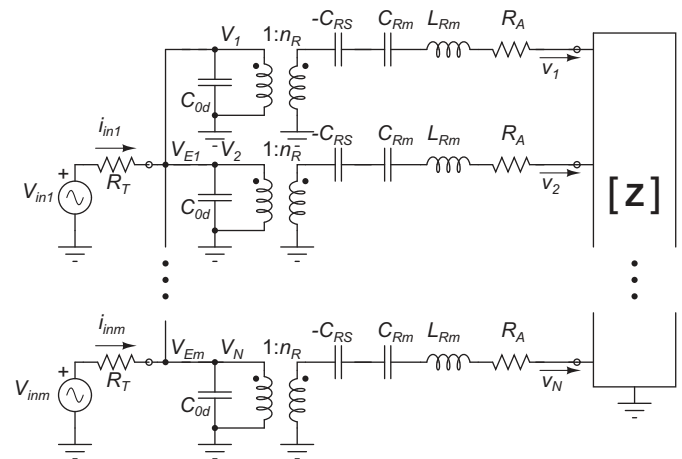

Fig. 2. Small-signal equivalent circuit of an array of CMUT cells immersed in a liquid medium. The plate velocity is modelled with the lumped *rms* velocity. m elements are driven by AC voltage sources $V_{in1}, V_{in2}, \cdots, V_{inm}$ each with a source resistance R_T.

small signal equivalent circuit using *rms* quantities as through and across variables [8]. This simple linear circuit only models the lowest order vibrational mode of the CMUT plate, it does

not predict the response at higher frequencies where higher order modes are excited or at large-signals where harmonics are generated. A series resistor, R_A, is added in the model to account for the mechanical loss. The mechanical ports of the $N = n \times m$ cells are connected to an N-port represented by the $N \times N$ $\mathbf{Z}$ matrix. Diagonal entries of $\mathbf{Z}$ matrix represent the self-radiation impedance [4] of the CMUT cells, while the off-diagonal entries [9] show the mutual-radiation impedance between the cells. The array elements are connected to m sinusoidal voltage sources, $V_{in1}, V_{in2}, \cdots, V_{inm}$, with source impedances of R_T.

We can formulate the problem as a set of N linear equations to be solved at each frequency point. If $\mathbf{V_{in}}$ and $\mathbf{v}$ are the $N \times 1$ column vector of drive voltages and cell velocities, we can write the N linear equations as a matrix equation:

$$n_R \mathbf{V_{in}} = \mathbf{\Psi}(\omega) \, \mathbf{v} \qquad \text{with} \qquad (1)$$

$$\mathbf{\Psi}(\omega) = [j\omega C_{0d} R_T \mathbf{J} + \mathbf{I}]\mathbf{M} + n_R^2 R_T \mathbf{J} \qquad (2)$$

where n_R is the electromechanical transformer turns ratio, $\mathbf{J}$ is an $N \times N$ cell-connection matrix, containing m all-ones matrices ($n \times n$ each) along its diagonal to describe the wiring of the cells, $\mathbf{I}$ is an $N \times N$ identity matrix. Diagonal entries of $N \times N$ $\mathbf{M}$ matrix has the mechanical part of the individual cell models and self-radiation impedance, and the off-diagonal entries contain the mutual-radiation impedance values. We can solve for individual cell velocities by inverting the $N \times N$ $\mathbf{\Psi}$ matrix:

$$\mathbf{v} = n_R \mathbf{\Psi}^{-1} \mathbf{V_{in}} \qquad (3)$$

We note that the matrices are not sparse, since the mutual impedance function is a slowly decaying function of separation. Hence the solution requires the inversion of a full-matrix of size $N \times N$ at every frequency.

III. ARRAY SIMULATIONS

We consider an array of 64×256 CMUT cells with radius a=45.7 μm. With t_m=1.92 μm, individual cells are resonant at 1.4 MHz. With t_{ge}=298nm, the collapse voltage under 1atm pressure is 55V. The cell models have a series resistor (R_A) to give a loss of 0.6 dB, which is found by comparisons with measurement results. We assume that the CMUT cells are biased with V_{DC}=50V. The cells are placed on a rectangular grid with a s=3 μm separation between the cells. The array contains m=64 elements with 64×4=256 cells in each, resulting in a size of 6.04mm×24.16mm. A cylindrical lens is placed on the array to provide focusing in one direction at a distance of 24mm. To provide focusing in the other direction, the phases of element excitations are adjusted so that the radiated acoustic waves focus at the same distance at the middle of the array. The solutions of matrix equation at seven different frequencies are shown as gray-scale patterns in Fig. 3.

The results indicate considerable variation in the velocities of the individual cells of an element, although they are excited in parallel. At lower frequencies, a standing wave pattern is
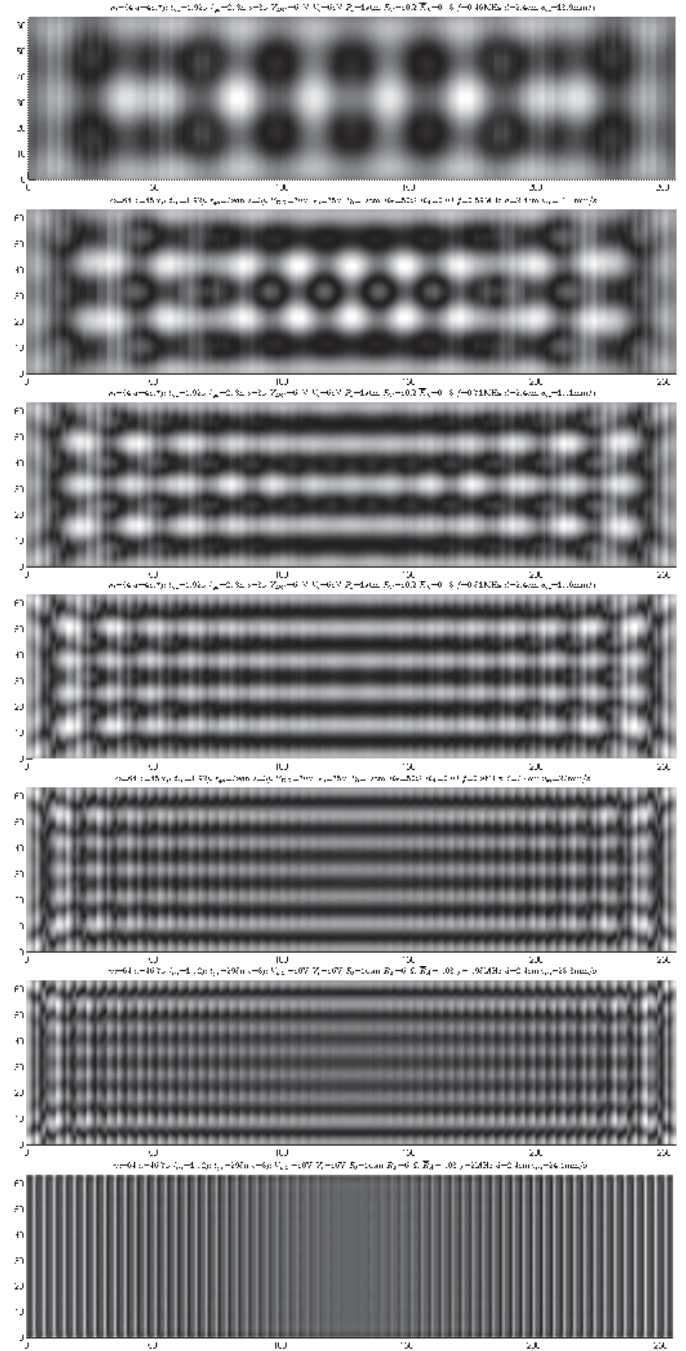

Fig. 3. Calculated velocity magnitude map of an array of 64×256 cells divided into 64 elements at 0.46, 0.59, 0.71, 0.81, 0.90, 0.98 and 2.00 MHz (from top to bottom). Dimensions and parameters: a=45.7 μm, t_m=1.92 μm, t_{ge}=298nm, R_A=0.03$\pi a^2 \rho_0 c_0$, s=3 μm, Y_0=320GPa, σ=0.263, ρ=3270kg/m^3, c_0=1500m/s, ρ_0=1000kg/m^3 and V_{DC}=50V. Elements are excited in such a way to focus at a distance of 24mm in the middle.

apparent.* At frequencies above 1.6 MHz (slightly above the resonance frequency of a single cell), the standing wave pattern is absent, but there are still uneven velocities within the cells of an element, due to unequal excitation in the neighboring

*The frequencies are chosen to give the highest standing-wave-ratio.

2014 IEEE International Ultrasonics Symposium Proceedings

elements or due to the edge effect. Those cells, which are on the edge of the element or the array, experience a significantly lower impedance. As a result, the displacement of the cells at the edge is more than the displacement of the cells in the middle.

IV. RAYLEIGH-BLOCH WAVES

It is known that periodically placed resonators on plane surface may support Rayleigh-Bloch (R-B) waves [10] along the surface. Linton and McIver [11] showed that these waves can exist in the absence of any incident waves.

For the purpose of demonstration, let us investigate the R-B waves on a single column of water immersed CMUT cells arranged on an infinitely long straight line and all driven by the same sinusoidal voltage V_{in}. We assume that an R-B wave exists, propagating along the straight line with a wavenumber of $k_B = \omega/v_B$. We represent this wave by $\exp(-jk_Bx)$ where x is the position of the cell center. For any cell, the solution is the same except for the phase factor of $\exp(-jk_Bx)$. With R_T=0 and $C_R = (C_{RS}-C_{Rm})/C_{Rm}C_{RS}$, we can write Eq. 2 as

$$\Psi(\omega) = j\omega L_{Rm} + \frac{1}{j\omega C_R} + Z_{RR}(ka)$$
$$+ \sum_{q=1}^{\infty} \left[\left(e^{-jqk_Bd} + e^{jqk_Bd}\right) Z_M(ka, qkd) \right] \quad (4)$$

where $d = 2a + s$ is the cell pitch, $k = \omega/c_0$ is the wavenumber in water, Z_{RR} and Z_M are the self and mutual radiation impedances. For a given ω, the cell velocities will be maximized, if the imaginary part of Ψ is zero. Using the approximate expressions for the mutual impedance, we find

$$Im\{\Psi(\omega)\} \approx \omega L_{Rm} - \frac{1}{\omega C_R} + Im\{Z_{RR}(ka)\}$$
$$+ 2A' \sum_{q=1}^{\infty} \left[\cos(qk_Bd)\frac{\cos(qkd)}{qkd} \right] = 0 \quad (5)$$

where $A' = \rho_0 c_o \pi a^2 \sum_{n=0}^{10} p_n(ka)^n$ [9]. We can simplify the infinite summation using the Mercator series to get an implicit analytic dispersion relation for R-B waves:

$$\omega L_{Rm} - \frac{1}{\omega C_R} + Im\{Z_{RR}(ka)\}$$
$$-A' \frac{\ln|1 - e^{j(k+k_B)d}| + \ln|1 - e^{j(k-k_B)d}|}{kd} = 0 \quad (6)$$

The dispersion curve for R-B waves in this structure is given in Fig. 4 for various values of cell separation distance s. The phase velocity for R-B waves is less than c_0=1500m/s, so they do not leak into the liquid medium. Notice the presence of a cut-off frequency above which no R-B waves exist. The cut-off arises from the Bragg condition, when the CMUT cell pitch is equal to a half wavelength of the R-B wave. For example, let us look at the s=3 μm curve in Fig. 4. The cut-off occurs at 1.6 MHz when v_B=300m/s. Hence the R-B wavelength is λ_B=188 μm. The cell pitch, d=2a+s=94.4 μm, corresponds nearly to the half-wavelength at the cut-off.

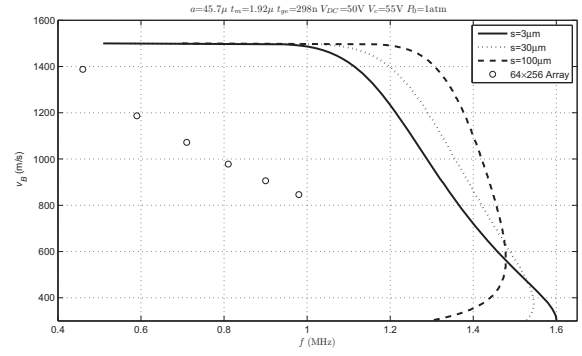Fig. 4. Dispersion curve for R-B waves on a single infinite column of the CMUT cells (cells are same as those given in Fig. 3) for s=3, 30 and 100 μm. CMUT cells are immersed in water. R-B wave velocity for the 64×256 array calculated from Eq. 7 is shown with circles.

When the array is of finite size, like the array we considered, the dispersion relation of R-B waves can only be found numerically. Moreover, reflection of R-B waves from the edges create standing-waves like a Fabry-Pérot resonator. Standing wave condition is satisfied when the R-B wavelength, λ_B, is an integer multiple of reflector separation D:

$$D = p\lambda_B \quad \text{or} \quad v_B = \frac{D}{p}f \quad \text{with} \quad p = 1, 2, \cdots \quad (7)$$

We can calculate v_B at different frequencies in Fig. 3 using Eq. 7. The results are shown in Fig. 4 as circles for p=2, 3, 4, 5, 6 and 7.

Simulations show that a moderate amount of loss in the CMUT cell is sufficient to eliminate high order modes, but low order modes remain even in the presence of significant loss. The arrays with small size are more prone to this undesired effect, while larger arrays suffer only from low order resonances.

V. TRANSFER FUNCTION AND PULSE RESPONSE

An ultrasonic imaging system requires a wide dynamic range, since losses from tissue attenuation can produce 80 to 100 dB variation in received signal amplitude [12]. The amount of the required dynamic range will depend on the delay from the initial excitation pulse. It is therefore a requirement that the transducer should not have long lasting resonances.

To assess the possible detrimental effects of R-B waves, we calculated the field pattern at the focus. We found no significant degradation in the point spread function due to R-B waves or velocity fluctuation in the cell velocities.

We also found the transfer function of the focusing array under consideration in the frequency domain. The transfer function magnitude and phase are plotted in Fig. 5. 3-dB bandwidth extends from 0.5 MHz to 5.5 MHz, corresponding to a center frequency of 3 MHz with 166% fractional bandwidth. It is seen that there is an oscillatory behavior in the magnitude and phase at low frequencies where the R-B waves are excited.

To observe the consequences of this fluctuation in the time domain, we calculated the pulse response using a Gaussian

2014 IEEE International Ultrasonics Symposium Proceedings

64×256 m=64 a=45.7μ t_m=1.92μ t_ge=298n s=3μ V_{DC}=50V V_c=55V P_0=1atm R_T=50Ω \overline{R}_A=0.03 f=15MHz d=2.4cm
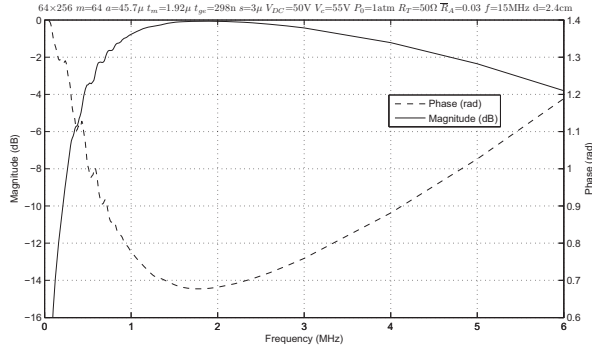
Fig. 5.   Transfer function of the 64×256 array.

pulse with a center frequency of 3 MHz and fractional bandwidth of 150%. The pulse response is shown in Fig. 6 on a dB scale to show the dynamic range of the system. The cells continue to vibrate at 7 μs limiting the dynamic range to 55 dB. At 25 μs the dynamic range is limited to 78 dB.

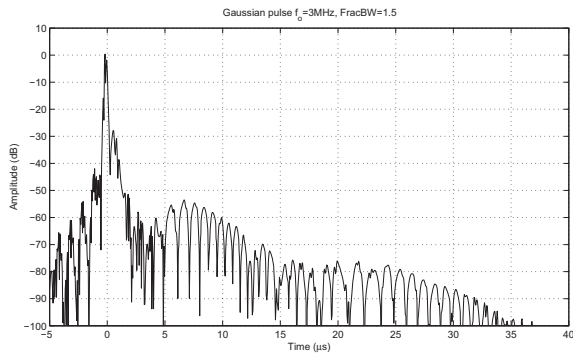Gaussian pulse f_o=3MHz, FracBW=1.5

Fig. 6.   Pulse response of the 64×256 array. Pulse has a center frequency of 3 MHz with a 150% fractional bandwidth.

VI. ELIMINATING RAYLEIGH-BLOCH WAVE RESONANCES

If the dynamic range offered by the CMUT array is not found satisfactory, it is possible to reduce R-B wave excitation, by introducing more loss in the CMUT cells. A loss of about 3 dB eliminates all resonances, except the lowest orders. This is not very desirable, since it degrades the output power as well as the noise figure of the CMUT probe.

Simulations indicate that introducing loss only at the edge cells of an array may be sufficient to significantly reduce the amplitude of the Fabry-Pérot resonances of R-B waves. Loss must be carefully adjusted in the edge cells to create a matched condition for R-B waves to prevent a reflection at the edges.

VII. CONCLUSIONS

The mechanical impedance of a typical CMUT cell in an array is small compared to the total radiation impedance seen by the cell. So, the behavior of the cell is determined mostly by the radiation impedance. Since the radiation impedance

depends heavily where the cell is located and what the neighboring cells are doing, the cell behavior in an array can be complicated.

Simulation results of arrays point out the presence of spurious resonances near the center frequency of individual cells. We show that these resonances, also observed experimentally, are due to Rayleigh-Bloch waves travelling laterally on the CMUT surface-liquid interface. For linearly placed CMUT cells, we derive an analytical expression for the dispersion relation of this wave. The highly dispersive Rayleigh-Bloch waves have a phase velocity slower than the sound speed in the liquid and they cannot exist above a cut-off frequency. The spurious resonances occur at frequencies when these waves reflect from the edges of the array and form standing waves similar to that in a Fabry-Pérot resonator. These resonances do not cause a significant degradation in the focus performance, but it degrades the impulse response and hence limits the dynamic range of an imaging system using the CMUT probe.

It is possible to diminish the amplitude of R-B wave Fabry-Pérot resonances by introducing loss only at the edge cells of an array.

REFERENCES

[1] X. Jin, O. Oralkan, F. L. Degertekin, and B. T. Khuri-Yakub, "Characterization of one-dimensional capacitive micromachined ultrasonic immersion transducer arrays," *IEEE Transactions on Ultrasonics, Ferroelectrics, and Frequency Control*, vol. 48, pp. 750–759, 2001.

[2] A. Caronti, A. Savoia, G. Caliano, and M. Pappalardo, "Acoustic coupling in capacitive microfabricated ultrasonic transducers: Modeling and experiments," *IEEE Transactions on Ultrasonics, Ferroelectrics, and Frequency Control*, vol. 52, pp. 2220–2234, 2005.

[3] K. K. Park, M. Kupnik, H. J. Lee, B. T. Khuri-Yakub, and I. O. Wygant, "Modeling and measuring the effects of mutual impedance on multi-cell CMUT configurations," in *Proceedings of the IEEE Ultrasonics Symposium*, 2010, pp. 431–434.

[4] M. N. Senlik, S. Olcum, H. Koymen, and A. Atalar, "Radiation impedance of an array of circular capacitive micromachined ultrasonic transducers," *IEEE Transactions on Ultrasonics, Ferroelectrics, and Frequency Control*, vol. 57, pp. 969–976, 2010.

[5] A. Rønnekleiv, "CMUT array modeling through free acoustic CMUT modes and analysis of the fluid-CMUT interface through Fourier transform methods," *IEEE Transactions on Ultrasonics, Ferroelectrics, and Frequency Control*, vol. 52, pp. 485–490, 2005.

[6] M. Wilm, A. Reinhardt, V. Laude, R. Armati, W. Daniau, and S. Ballandras, "Three dimensional modelling of micromachined-utrasonic-transducer arrays operating in water," *Ultrasonics*, vol. 43, pp. 457–465, 2005.

[7] M. Berthillier, P. Le Moal, and J. Lardiès, "Dynamic and acoustic modeling of capacitive micromachined ultrasonic transducers," in *Proceedings of the IEEE Ultrasonics Symposium*, 2011, pp. 608–611.

[8] H. Koymen, A. Atalar, E. Aydogdu, C. Kocabas, H. K. Oguz, S. Olcum, A. Ozgurluk, and A. Unlugedik, "An improved lumped element nonlinear circuit model for a circular CMUT cell," *IEEE Transactions on Ultrasonics, Ferroelectrics, and Frequency Control*, vol. 59, pp. 1791–1799, 2012.

[9] H. K. Oguz, A. Atalar, and H. Koymen, "Equivalent circuit-based analysis of CMUT cell dynamics in arrays," *IEEE Transactions on Ultrasonics, Ferroelectrics, and Frequency Control*, vol. 60, pp. 1016–1023, 2013.

[10] R. Porter and D. Evans, "Rayleigh-Bloch surface waves along periodic gratings and their connection with trapped modes in waveguides," *J. Fluid Mech.*, vol. 386, pp. 233–258, 1999.

[11] C. M. Linton and M. McIver, "The existence of Rayleigh-Bloch surface waves," *J. Fluid Mech.*, vol. 470, pp. 85–90, 2002.

[12] M. E. Schafer and P. A. Lewin, "Influence of front-end hardware on digital ultrasonic imaging," *IEEE Trans. on Sonics and Ultrasonics*, vol. 31, pp. 295–306, 1984.